

PAPER • OPEN ACCESS

## Hydrogen diffusion in Zr-2.5Nb pressure tubes specimens between 300°C-400°C by in-situ neutron imaging experiments

To cite this article: V.M. Stella *et al* 2023 *J. Phys.: Conf. Ser.* **2605** 012037

View the [article online](#) for updates and enhancements.

You may also like

- [High spatial resolution neutron detection technique based on Commercial Off-The-Shelf CMOS image sensors covered with NaGdF<sub>4</sub> nanoparticles](#)  
M. Pérez, E.D. Martínez, J. Lipovetzky et al.
- [FIB-TEM y FIB-SEM Characterization of the Electrode/Electrolyte Interface in Solid Oxide Fuel Cell Materials](#)  
Analia L. Soldati, Laura Baqué, Horacio Troiani et al.
- [The generalized Wiener process II: Finite systems](#)  
Adrián A Budini and M O Cáceres

**PRIME**  
PACIFIC RIM MEETING  
ON ELECTROCHEMICAL  
AND SOLID STATE SCIENCE

HONOLULU, HI  
Oct 6–11, 2024

Abstract submission deadline:  
**April 12, 2024**

Learn more and submit!

**Joint Meeting of**  
The Electrochemical Society  
•  
The Electrochemical Society of Japan  
•  
Korea Electrochemical Society

## Hydrogen diffusion in Zr-2.5Nb pressure tubes specimens between 300°C-400°C by in-situ neutron imaging experiments

V.M. Stella<sup>1,2</sup>, S.R. Soria<sup>3,4</sup>, A. Gomez<sup>5</sup>, M. Grosse<sup>6</sup>, M. Schulz<sup>7</sup> and J. R. Santisteban<sup>2,4</sup>

<sup>1</sup>Instituto Balseiro, Centro Atómico Bariloche, Av. Bustillo 9500, 8400 S. C. de Bariloche, Argentina.

<sup>2</sup>Comisión Nacional de Energía Atómica, Laboratorio Argentino de Haces de Neutrones, Argentina.

<sup>3</sup>División Física de Metales, Centro Atómico Bariloche, Av. Bustillo 9500, 8400 S. C. de Bariloche, Argentina.

<sup>4</sup>CONICET (Consejo Nacional de Investigaciones Científicas y Técnicas), Argentina.

<sup>5</sup>Departamento Tecnología de Aleaciones de Circonio, Centro Atómico Ezeiza, Cam. Real Presbítero González y Aragón 15, B1802 Ezeiza, Argentina.

<sup>6</sup>Institut für Angewandte Materialien, Karlsruher Institut für Technologie, 76128 Karlsruhe, Germany.

<sup>7</sup>Heinz Maier-Leibnitz Zentrum (MLZ) FRM II, Technische Universität München, Lichtenbergstr. 1, 85747 Garching, Germany.

E-mail: valentina.stella@ib.edu.ar

**Abstract.** Zirconium (Zr) alloys are widely used in nuclear power plants as fuel cladding and are susceptible to hydrogen (H) degradation. For long operational service, Zr-based components can suffer a mechanism known as Delayed Hydride Cracking (DHC) associated to an increase of the crack propagation velocity by the re-orientation and precipitation of Zr hydride. In this process, the H mobility has a great influence. In the present work, the isothermal diffusion of H in Zr-2.5%Nb specimens obtained from a CANDU pressure tube were studied at consecutive temperatures of 300°C, 350°C, 375°C and 400°C. H content and mobility were quantified by in-situ neutron imaging experiments performed on ANTARES, the cold neutron imaging facility of FRM II. The time evolution of the H concentration across the specimen allowed the determination of diffusion coefficients, and an assessment of the limitations of existing models commonly used to describe H diffusion.



## 1. Introduction

Zirconium (Zr) alloys are used in nuclear power plants as fuel cladding due to an excellent combination of mechanical resistance, corrosion resistance and very low neutron absorption. The heat produced by the nuclear reactions is evacuated using coolant water which, at high temperature and pressure, can produce oxidation on the fuel cladding with the subsequent release of hydrogen (H). Due to its low terminal solid solubility (TSS), the H incorporated by the Zr alloy forms a brittle phase of Zr hydride that tends to be located on stress concentrators such as crack tips or surface flaws on the fuel cladding. Under the presence of mechanical stress, hydrides can be re-oriented in the direction of the crack, accelerating crack propagation as shown in figures 1 and 2. This phenomenon is known as Delayed Hydride Cracking (DHC) and reduce Zr-based components service life [1].

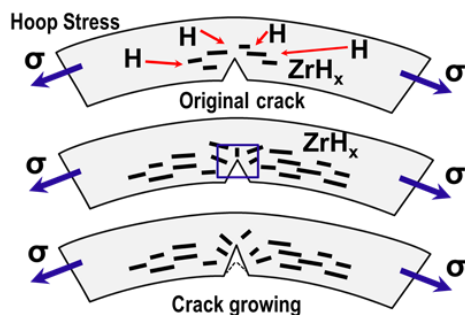


**Figure 1.** Scheme illustrative of crack growth due to hydride precipitation and reorientation.

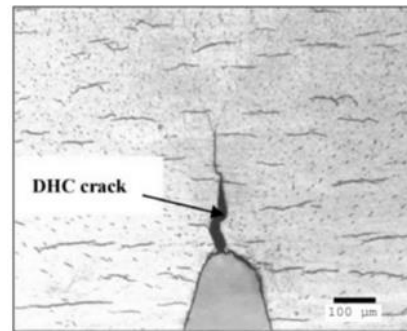


**Figure 2.** Micrograph of DHC process with the crack propagated by a hydride reoriented in the crack direction [2].

H migration to the crack tip in DHC process is governed by H diffusion. Then, proper quantification of the H diffusion coefficient is an important issue for the safety operation of nuclear power plants. Pressure tubes (PTs) in CANDU power plants are made of a Zr-2.5%Nb alloy (ZrNb in the following.). ZrNb is a biphasic alloy formed by  $\alpha$ -Zr phase and  $\beta$ -Zr phase that have a hexagonal close-packed (hcp) and body-centered cubic (bcc) crystallographic structures, respectively. As H diffusion is faster in the bcc phase than in the hcp phase, H diffusivity in bi-phase alloys depends of the spatial distribution of the phases and the phase fractions. The microstructure of the  $\beta$ -phase can be affected by heat treatments. As an example, in PTs annealed for 1 h at 550°C, the  $\beta$ -phase separates in two phases, one is completely decomposed (discontinuous)  $\beta_2$ -phase and segments of  $\beta$ -phase that remains relatively intact ( $\beta_1$ ) [3]. Then, annealing treatments performed during production or operation of PTs could reduce the H mobility in the material due to the formation of  $\beta_2$ -phase.

Neutrons are excellent to study the presence of H in metals due to the differences in attenuation coefficient ( $\Sigma$ ) provides good contrast between hydrides and metal alloys [4]. Then, NI emerges as a suitable technique to study the redistribution of H in Zr alloys. After proper calibration, neutron imaging (NI) allows non-destructive, quantitative analysis of processes in-situ and in-operando.

In the present work, the diffusion coefficient of H in samples of ZrNb obtained from CANDU pressure tubes was analysed. For this purpose, in-situ thermal treatment consisting of sequential annealing of specimens at temperatures of 300°C, 350°C, 375°C and 400°C were performed.

## 2. Experimental method

Two samples of 10x10x4 mm<sup>3</sup> were machined from a ZrNb pressure tubes produced in Ezeiza Atomic Center, Argentina, for the Embalse nuclear power plant life extension project [5]. One of the samples was annealed at 600°C during 4 h to produce the discontinuous  $\beta_2$ -phase which was named as PT-T. The remaining pristine sample from pressure tube was named PT. A hydride layer was produced in one of the square faces of the sample, hence allowing the diffusion of H from the hydride layer into the ZrNb material along a 4 mm diffusion length. The hydride layer was incorporated by cathodic charging in an

aqueous solution of sulphuric acid (200 ml H<sub>2</sub>O + 5ml H<sub>2</sub>SO<sub>4</sub>) at 85°C during 24-30 h, producing hydride layers on all six faces of the specimens being five of them removed by mechanical machining. The samples were annealed at fixed temperatures during the NI experiments with the neutron beam direction parallel to the hydride layer face, hence traversing 10 mm of material.

NI experiments were carried out in the ANTARES, the cold neutron imaging facility of FRM II in Garching, Germany [6]. Experiments were performed using a collimation ratio L/D of 500 while the images were acquired using a ANDOR cooled CCD and Gd<sub>2</sub>O<sub>2</sub>S scintillator plate of 20 µm thickness with a field-of-view (FoV) of 40 x 40 mm<sup>2</sup>. In-situ thermal treatments were performed using a heating holder made of aluminum alloy. Two cylindrical heating cartridges of 5x35 mm<sup>2</sup> with an electrical power of 50 W were used to maintain them at a certain temperature the samples during irradiation. The temperature control was carried out employing two resistive sensors type RTD Pt1000 (Resistance Temperature Detector), located at opposite extremes of the heating plate. It was controlled that the temperature variation between the extremes of the heating plate does not exceed 2°C. The heating plate allows locating six samples at the same time. Samples were covered by an Al plate mounted fixed to the heating plate using Ti screws. The heating holder is shown in figure 3 while the temperature curve measured is presented in figure 4. The holder was located at 12 mm of the scintillator plate obtaining a pixel size of 33 µm. NI were acquired every 30 s and averaging forming stacks of 30 images, obtaining time steps of 15 min. The in-situ thermal treatment (TT) consists of different temperature steps at 300°C, 350°C, 375°C and 400°C during 210 min, 120 min, 60 min and 120 min, respectively. Ordinate axis in figure 4 indicates the total time that start in the beginning of the first temperature step at 300°C.

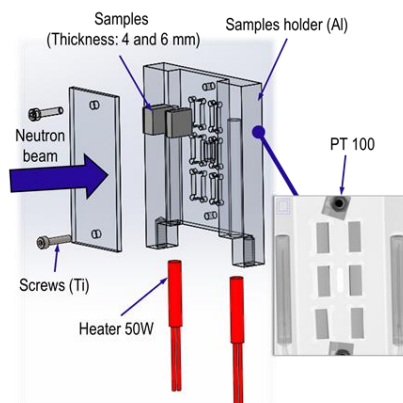


**Figure 3.** Diagram of the sample holder used and neutron imaging of this with samples.

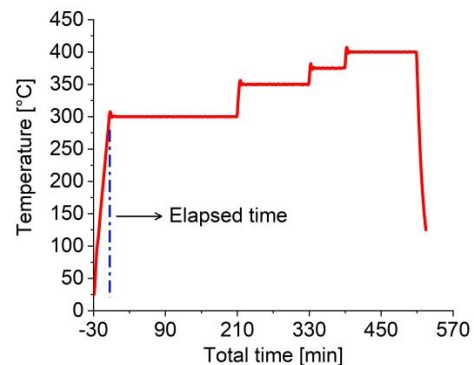


**Figure 4.** Experimental temperature ramps measured during the experiments.

Neutron transmission ( $Tr$ ) was calculated after the flat field and dark current correction. Moreover, an additional correction was performed to extract the attenuation of the heating holder. Buitrago *et al.* [7] determined the linear relationship between attenuation  $\Sigma$  and H content for different Zr alloys. For this, calibration samples with homogeneous H contents were measured by neutron imaging and compared with the results of hot vacuum extraction. Grosse *et al.* [8] found that in the linear relationship between H content and  $\Sigma$ , the slope depends of the configuration factors such as the neutron spectrum, the L/D factor and the detection system used (scintillator plate, digital camera). On the other hand, the ordinate to the origin must be corrected because it is affected by the experimental setup used, e.g., different types of sample holders, heating elements and cryostats, among others. As in the present experiments the instrument configuration was the same as the employed in Ref [6], the new ordinate should be determined. This was measured mounting the calibration samples into the heating holder. Finally, the relationship between the H content and  $\Sigma$  is presented in equation (1) that was used to determine the H content maps of the samples.

$$H(\text{wt. ppm}) = 4347,82[\text{wt. ppm} \cdot \text{cm}] \cdot \Sigma[\text{cm}^{-1}] - 929,13[\text{wt. ppm}] \quad (1)$$

### 3. Results and discussion

Figure 5 presents the H content maps of PT sample at different times during the experiment, which shows no dependence on the vertical direction. H content profiles normal to the hydride layer were evaluated by averaging the 6 mm central region identified by the yellow box in figure 5. Figure 6 shows the resulting H content profiles after total times of 210 min (300°C) and 255 min (350°C).

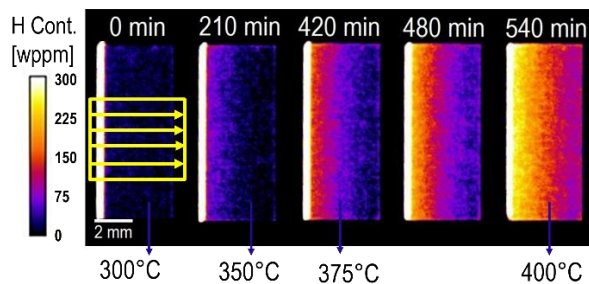


**Figure 5.** H content maps for the PT sample. Region marked indicate the zone to obtain the H content profiles.

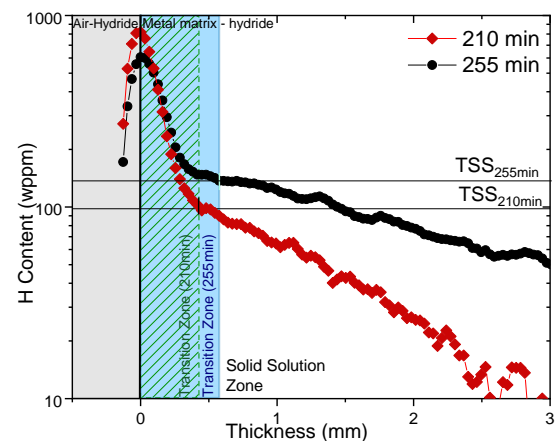


**Figure 6.** H content profile in PT sample at total times of 180 min (300°C) and 255 min (350°C).

In the profiles on figure 6, three zones had been distinguished during the analysis:

- **Hydride layer.** This is well distinguishable in the profiles as a high peak of H content at the beginning of the curve surrounded by two interfaces: a) air-hydride and b) metal matrix-hydride. This corresponds to the hydride formed in the samples during the cathodic charge that acts as H source.
- **Diffusion zone.** In this region, the H is present in solid solution during the annealing at the different temperature steps. Here is where the diffusive process can be described by applying the Fick's laws. At the start of the annealing, the diffusion zone is located immediately after the hydride layer. The limit or boundary between the hydride layer and the diffusion zone coincides with the position where the H content is equal to the terminal solid solubility (TSS) of H at the temperature step analyzed. However, over time a third zone appears between the hydride layer and the solid solution. This is described in the following.
- **Transition zone.** This zone is developed between the two zones described above during the TT. This could be related to the presence of hydrides partially dissolve originated from the initial hydride layer [7]. The limits of this zone must be defined between the beginning of the solid solution zone that corresponds to the point where the H concentration is equal to the TSS for the temperature step of the sample and the end of the hydride layer. The boundary with the hydride layer is established as the first inflection point of the curve after the maximum.

H content profiles at different total times from the beginning of the TT are shown in figures 7 and 8 for PT-T and PT samples, respectively. TSS values were determined from the inflexion point and the plateau formed after the transition zone [9] and they are indicated in figures 7 and 8. TSS values obtained increase with the temperature increasing, and are similar to those reported in the literature for the PT sample [10]. On the other hand, TSS values for PT-T sample were lower and that can be related to changes in the microstructure. The H solubility is affected by the spatial distribution of hydrides and the

thermal treatment can promote a finer hydride distribution that they retain greater elastic deformation, thus reducing the value of enthalpy formation in the TSS values for dissolution and precipitation [11].

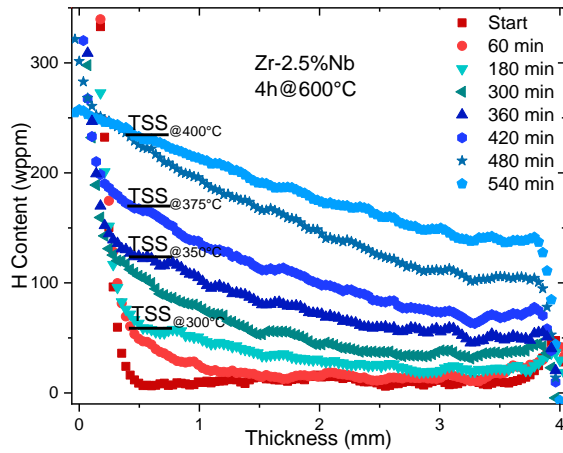


**Figure 7.** Evolution of the H content profiles in PT-T sample.

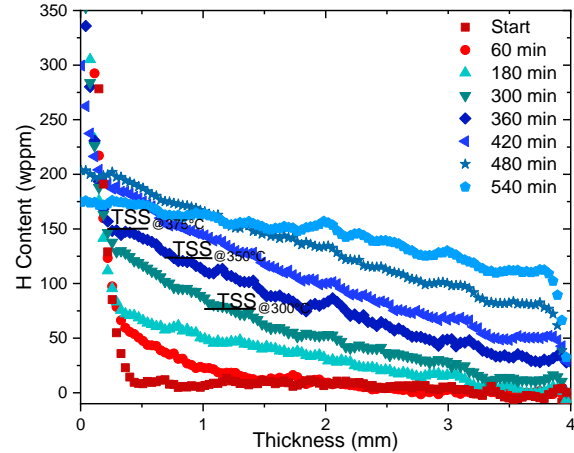


**Figure 8.** Evolution of the H content profiles in PT sample.

In figures 7 and 8 is observed that H diffuses from the hydride layer into the thickness of the sample. To quantify the mobility of the H atoms, the diffusion coefficient  $D$  was analysed.  $D$  was obtained fitting the H content profiles following the Fick's second law. Firstly, the solution for a semi-infinite medium in a one-dimensional geometry was used, that considers the hydride layer equivalent to an infinite H source. This model is described using the complementary error function-type following the equation (2), where  $C_0$  is the initial H content of the sample,  $D$  the diffusion coefficient, TSS the terminal solid solubility of the H,  $x$  the position into the sample and the temperature step analysed and  $t$  the time elapsed from the beginning of the annealing at the temperature step considered. H profiles fitted for the PT-T sample are shown in figure 9.

$$C(x,t) = C_0 + (C_0 - TSS) \cdot \operatorname{erfc}\left(\frac{x}{2\sqrt{D \cdot t}}\right) \quad (2)$$

In the PT sample, reaching 400°C temperature step this model was not valid due to after 60 min at this temperature (480 min curve in figure 8), the maximum H content in the peak layer was 270 wt. ppm while the TSS expected at this temperature is close to that value, in the order of 210 wt. ppm [10]. This assumption was validated to the end of the step at 400°C when all H content in the samples were lower than the theoretical TSS and the difference between the maximum and minimum H concentration was in the order of 25 wt. ppm. Then, the infinite source model is not adequate for this temperature annealing. For this reason, a Gaussian diffusion was adopted for this temperature step considering that H content of the source is decreasing in the time which is described by equation (3), where  $M$  is original H concentration on the surface deposited during the formation of the hydride layer.

In order to study the temporal evolution of  $D$ , the diffusivities obtained of the PT-T sample as a function of the elapsed time during isothermal annealing are shown in figure 10. It can be observed that  $D$  decay with the elapsed time, being the values relatively constant only in the annealing performed at 300°C. This decay of the  $D$  values can be related to the kinetics dissolution of the hydrides [12]. These values were calculated analysing each time step independently from the previous and the next steps. In this way, the second Fick's second law, which considers a  $D$  parameter constant in the time, is still valid.

$$C(x,t) = \frac{M}{\sqrt{\pi \cdot D \cdot t}} \cdot \exp\left(\frac{-x^2}{4 \cdot D \cdot t}\right) \quad (3)$$

D values obtained in each temperature step for both samples are showed in the Table 1. Steady D coefficients were obtained after the first 60 min in each temperature step. This criterion was based on the work of Kearns [12] in Zircaloy 4 alloys finding that, after this time, the dissolution kinetics of the hydrides is homogeneous. The effects of the time dependence observed in the dissolution of the hydrides platelets that produces a time dependence in the D coefficient as well as the existence of a transition layer related to the partial dissolution of the initial hydride layer forming the transitions region. The existence of the kinetics effects in the H diffusion cannot be explained using the common diffusion models determined by the Fick's laws.

In Table 1 is noted that D is lower in the PT-T sample than in PT sample, demonstrating that the thermal treatment performed at 600°C during 4 h certainly changes the microstructure of the material, affecting the H diffusion paths. On the other hand, D at 400°C for the PT sample is four times the obtained in the PT-T sample. Shiman *et al.* [13] analyses the evolution of H solubility in ZrNb pressure tube during thermal cycling between 100–400°C. They found that at 400°C, in diffraction spectra the hydride peaks disappeared, indicating a full dissolution of the hydride phase at this temperature. A similar effect is observed in the PT samples analysed in the present work that is supported by the H content profiles shown in figure after a total time of 540 min (400°C).

**Table 1.** Steady diffusion coefficients obtained from the fitting of the experimental H concentration profiles, after the first 60 min of TT.

Temperature [°C]	D of PT-T sample [m <sup>2</sup> /s]	D of PT sample [m <sup>2</sup> /s]
300	$(0,6\pm0,3)\times10^{-10}$	$(1,7\pm0,4)\times10^{-10}$
350	$(2,1\pm0,9)\times10^{-10}$	$(5,5\pm0,3)\times10^{-10}$
375	$(5\pm4)\times10^{-10}$	$(9,8\pm0,3)\times10^{-10}$
400	$(6\pm3)\times10^{-10}$	$(24\pm14)\times10^{-10}$

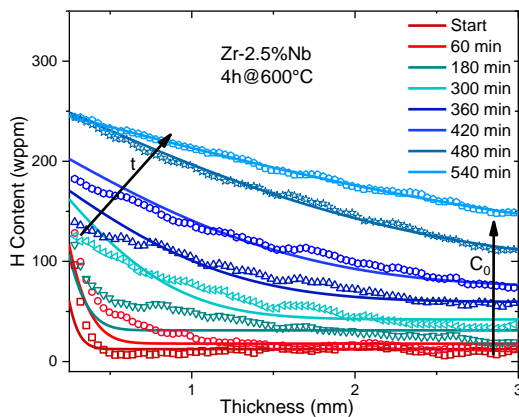


**Figure 9.** H profiles fitted from the curves in figure 7 for PT-T sample.

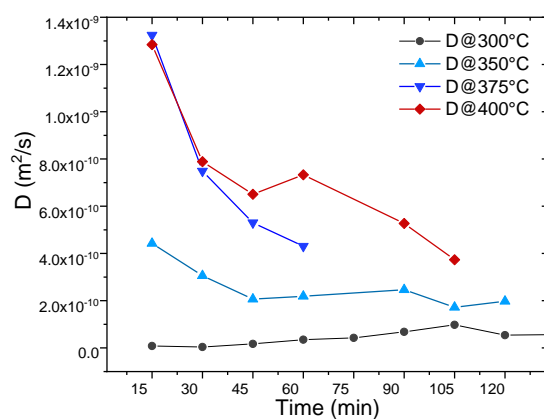


**Figure 10.** Time evolution of D at different temperatures in PT sample.

As mentioned above, Griffiths [3] found that a heat treatment at 475°C during 1 h causes the decomposition of the  $\beta$ -phase in Zr-2.5%Nb PT specimens. Both samples analyzed come from the same PT, with the difference that one sample had a previous treated for 4 h at 600°C that changes its microstructure. Due the  $\beta$ -phase has a higher H diffusivity as well as considerably higher solubility of H [3] than the  $\alpha$ -phase, the previous thermal treatment originates the changes reported in the present work in D and TSS value. Then, it can be concluded that the realization of this type of annealing reduce

the H incorporation into Zr-2.5%Nb alloys, although it also impacts on the mechanical properties of the alloy.

#### 4. Conclusions

From the experimental results obtained and discussed in the previous sections, the main conclusions obtained in the present work were:

- The NI technique is an adequate technique to study the H diffusion process in Zr-based alloys. In these experiments, a pixel size of 33  $\mu\text{m}$  with temporal steps of 15 min were employed during in-situ thermal treatments. This kind of experiments cannot be performed using others techniques.
- The existence of a transition zone was observed between the hydride layer formed during the cathodic charge (H source) and the solid solution region.
- A previous thermal treatment at 600°C during 4 h provides a significant decrease in the H diffusivity in Zr-2.5%Nb pressure tube samples. This effect is originated by the decomposition of the  $\beta$ -Zr phase.
- TSS values change due to the presence of this previous thermal treatment that could be related to the finer hydride distribution.
- In the case of the pressure tube sample without the previous thermal treatment, H mobility was very high and the system cannot be modeled as the infinite H source at 400°C step. Then, it was necessary to model the system using a finite source model (Gaussian function).
- H diffusion coefficients obtained in each time step presents a temporal decay. Moreover, the common diffusion models determined by the Fick's laws are not enough to analyze the H diffusion in Zr alloys. This could be related to the activation time needed in the hydride dissolution mechanism.

#### References

- [1] Singh R N, Kumar N, Kishore R, Roychaudhury S, Sinha T K and Kashyap B P 2002 *J. Nucl. Mater.* **304** 189.
- [2] Kim Y S, Ahn S B and Cheong Y M 2007 *J. Alloys Compd.* **429** 221.
- [3] Griffiths M, Winegar J E and Buyers A 2008 *J. Nucl. Mater.* **383** 28.
- [4] Pfrezschner B, Schaupp T and Griesche A 2019 *Corrosion* **75** 903.
- [5] Poletto G and Cepero R V 2022 *Pressurized Heavy Water Reactors* (Amsterdam: Elsevier) 399.
- [6] Schulz M and Schillinger B 2015 *JLSRF* **1** A17.
- [7] Buitrago N L, Santisteban J R, Tartaglione A, Marín J, Barrow L, Daymond M R, ... and Kabra S 2018 *J. Nucl. Mater.* **503** 98.
- [8] Grosse M, Van den Berg M, Goulet C, Lehmann E and Schillinger B 2011 *Nucl. Instrum. Methods Phys. Res., Sect. A* **651** 253.
- [9] Santisteban J R, Buitrago N L, Riffo A M, Soria S R, Baruj A L, Schulz M, ... and Daymond M R 2022 *J. Nucl. Mater.* **561** 153547.
- [10] Parodi S A, Ponzoni L M, De Las Heras M E, Mieza J I and Domizzi G 2016 *J. Nucl. Mater.* **477** 305.
- [11] Khatamian D 2003 *J. Alloys Compd.* **356–357** 22.
- [12] Kearns J J 1968 *J. Nucl. Mater.* **27** 64.
- [13] Shiman O, Tulk E and Daymond M R 2016. *Measurement of hydride precipitation and dissolution kinetics using synchrotron X-rays*. In Pressure Vessels and Piping Conference 50350, V01AT01A052. ASME.